Compton process in intense short laser pulses

K. Krajewska* and J. Z. Kamiński
Institute of Theoretical Physics, Faculty of Physics, University of Warsaw, Hoża 69, PL-00-681 Warsaw, Poland
(Received 28 March 2012; published 4 June 2012)

The spectra of Compton radiation emitted during electron scattering off an intense laser beam are calculated using the framework of strong-field quantum electrodynamics. We model these intense laser beams as finite length plane-wave-fronted pulses, similar to Neville and Rohrlich [Phys. Rev. D **3**, 1692 (1971)], or as trains of such pulses. Expressions for energy and angular distributions of Compton photons are derived such that a comparison of both situations becomes meaningful. Comparing frequency distributions for both an isolated laser pulse and a laser pulse train, we find a very good agreement between the results for long pulse durations which breaks down, however, for ultrashort laser pulses. The dependence of angular distributions of emitted radiation on a pulse duration is also investigated. Pronounced asymmetries of angular distributions are found for very short laser pulses, which gradually disappear with increasing the number of laser field oscillations. Those asymmetries are attributed to asymmetries of the vector potential describing an incident laser beam.

DOI: 10.1103/PhysRevA.85.062102 PACS number(s): 12.20.Ds, 12.90.+b, 42.55.Vc, 13.40.−f

I. INTRODUCTION

Compton scattering of a laser beam with a relativistic electron beam has become an efficient source of highly polarized, intense x-ray and γ-ray radiations. These monoenergetic and tunable Compton photon beams find numerous industrial, medical, and scientific applications. In particular, they bring a great deal of attention in the view of future colliders such as the International Linear Collider (ILC) [1], the Compact Linear Collider (CLIC) [2], and the Super B [3], which are planned to use the Compton γ rays to produce highly polarized positrons. Taking into account those various applications and research interests, it becomes of great importance to predict theoretically spectral and spatial distributions of Compton photon beams, and to control their properties using the incident beam parameters.

The hypothesis of a wavelength shift of x rays scattered by a free electron at rest has been put forward by Compton in Ref. [4], and proved by himself experimentally [5]. Following theoretical investigations have been focused on the so-called *linear Compton scattering* [6–11]. However, in extremely intense laser fields the scattering can occur in a nonlinear regime; the process known as the *nonlinear Compton scattering*. For the development of related theoretical studies, the reader is referred to a recent review by Ehlotzky and co-authors [12]. In brief, in a majority of works concerning the nonlinear Compton process, the incident laser beam has been described as a monochromatic plane wave field which enables one to fully account for the electron–laser-beam interaction using standard methods of strong-field quantum electrodynamics (QED) (see, for instance, [12–16] and references quoted therein). The first analysis that goes beyond the monochromatic plane-wave approximation when analyzing the nonlinear Compton scattering that we are aware of was by Neville and Rohrlich [17]. By generalizing the usual strong-field QED methods to account for a finite length plane-wave-fronted pulse, the authors considered the Compton scattering by a Klein-Gordon particle. Although the method proposed in [17] allows one to consider QED processes in laser pulses of an arbitrary duration and strength it has not had a big impact until very recently. Only very few papers on the scattering of a Dirac particle by a shaped laser pulse can be found in the literature. There is a paper by Narozhny and Fofanov [18] who have considered a situation when a driving laser pulse is still sufficiently long to allow one to simplify the problem significantly. In Ref. [19], the same approach has been persuaded in the context of a resonant Compton scattering. However, for intense few-cycle laser pulses which are used nowadays in experimental setups, a more adequate treatment of the temporal structure of an incident laser pulse is necessary. This has been offered in very recent papers [20–25] using the approach of Neville and Rohrlich [17].

In Ref. [20], Boca and Florescu have formulated the formalism for the nonlinear Compton scattering based on temporally shaped Volkov solutions for a Dirac particle. The calculated spectral distributions of Compton photons were compared for different pulse shapes and pulse durations. In the limit of a long pulse, these results coincide with the results of [18] showing no significant dependence on the precise form of the laser pulse. On the other hand, for short laser pulses pronounced carrier-envelope phase effects in spectral distributions of the Compton photons were demonstrated in [20,22]. A complementary study for single-cycle laser pulses was presented in [24], whereas the emphasis on a comparison with the *nonlinear Thomson scattering* (for reviews, see, for instance [26,27]) was put in Refs. [21,23,25]. All these theoretical works follow various related experiments. Experimentally, the nonlinear Compton scattering of relativistic electrons by an intense laser pulse has been observed for the first time by Englert and Rinehart [28]. In another experiment, the transition between the Thomson and Compton regimes of electron scattering has been reported [29]. However, the most prominent experiment showing nonlinear effects in the Compton scattering is the SLAC experiment [30,31] in which the fourth harmonic of the Compton radiation was detected.

Using the approach of Neville and Rohrlich [17], developed recently by Boca and Florescu [20], we shall consider in this paper the Compton scattering of an electron by a strong temporally shaped laser field. Our focus here is to develop new

*katarzyna.krajewska@fuw.edu.pl

theoretical and numerical methods to describe the situation when the incident laser field represents either an isolated laser pulse or a train of such pulses. The sensitivity of both spectral and angular distributions of the Compton radiation to a laser pulse duration will be studied in this paper in great detail.

Our paper is organized as follows. In Sec. II, we shall introduce the theory of Compton scattering of electrons by a temporally shaped ultrastrong laser beam. Two cases will be considered, when the laser beam is represented by a train of laser pulses (Sec. II A) and by an individual laser pulse (Sec. II B). In each case, a distribution of emitted radiation energy will be defined such that a comparison between the two situations is possible. In Sec. III, we shall define a laser pulse shape that will be used in our numerical calculations. In Sec. IV, we will analyze frequency distributions of Compton photons for different pulse durations. The results for an isolated laser pulse, a train of laser pulses, and for a monochromatic laser field will be compared. Angular distributions of emitted radiation for a single laser pulse will be shown in Sec. V. The emphasis will be put there on asymmetries in angular distributions which are observed for Compton processes induced by ultrashort laser pulses. Section VI will then be devoted to a summary of our results and to some final remarks.

Throughout the paper, we use the following mathematical convention and notation. In formulas, we keep $\hbar = 1$, however, our numerical results are presented in relativistic units such that $c = m_{\rm e} = 1$, where $m_{\rm e}$ is the electron mass. We write $a \cdot b = a^\mu b_\mu (\mu = 0,1,2,3)$ for a product of any two four-vectors a and b, and $\not{a} = \gamma \cdot a = \gamma^\mu a_\mu$ where γ^μ are the Dirac gamma matrices. In the following, the Einstein summation convention is used.

II. THEORY

Using the S-matrix formalism, we find that in the lowest order of perturbation theory, the probability amplitude for the Compton process $e^-_{\boldsymbol{p}_{\rm i}\lambda_{\rm i}} \to e^-_{\boldsymbol{p}_{\rm f}\lambda_{\rm f}} + \gamma_{\boldsymbol{K}\sigma}$, with the initial and final electron momenta and spin polarizations $\boldsymbol{p}_{\rm i}\lambda_{\rm i}$ and $\boldsymbol{p}_{\rm f}\lambda_{\rm f}$, respectively, equals

$$\mathcal{A}\big(e^-_{\boldsymbol{p}_{\rm i}\lambda_{\rm i}} \to e^-_{\boldsymbol{p}_{\rm f}\lambda_{\rm f}} + \gamma_{\boldsymbol{K}\sigma}\big) = -ie \int d^4x\, j^{(++)}_{\boldsymbol{p}_{\rm f}\lambda_{\rm f},\boldsymbol{p}_{\rm i}\lambda_{\rm i}}(x) \cdot A^{(-)}_{\boldsymbol{K}\sigma}(x), \tag{1}$$

where $\boldsymbol{K}\sigma$ denotes the Compton photon momentum and polarization. In the above equation,

$$A^{(-)}_{\boldsymbol{K}\sigma}(x) = \sqrt{\frac{1}{2\varepsilon_0 \omega_{\boldsymbol{K}} V}}\, \varepsilon^*_{\boldsymbol{K}\sigma} e^{iK\cdot x}, \tag{2}$$

where V is the quantization volume, ε_0 is the vacuum electric permittivity, $\omega_{\boldsymbol{K}} = cK^0 = c|\boldsymbol{K}|$ $(K \cdot K = 0)$, and $\varepsilon_{\boldsymbol{K}\sigma} = (0,\boldsymbol{\varepsilon}_{\boldsymbol{K}\sigma})$ is the polarization four-vector satisfying the conditions,

$$K \cdot \varepsilon_{\boldsymbol{K}\sigma} = 0, \quad \varepsilon_{\boldsymbol{K}\sigma} \cdot \varepsilon_{\boldsymbol{K}\sigma'} = -\delta_{\sigma\sigma'}, \tag{3}$$

for $\sigma,\sigma' = 1,2$. Moreover, $j^{(++)}_{\boldsymbol{p}_{\rm f}\lambda_{\rm f},\boldsymbol{p}_{\rm i}\lambda_{\rm i}}(x)$ (pluses indicate that we deal with particles of positive energy) is the matrix element of the electron current operator with its ν component equal to

$$\big[j^{(++)}_{\boldsymbol{p}_{\rm f}\lambda_{\rm f},\boldsymbol{p}_{\rm i}\lambda_{\rm i}}(x)\big]^\nu = \bar{\psi}^{(+)}_{\boldsymbol{p}_{\rm f}\lambda_{\rm f}}(x)\gamma^\nu \psi^{(+)}_{\boldsymbol{p}_{\rm i}\lambda_{\rm i}}(x). \tag{4}$$

Here, $\psi^{(+)}_{\boldsymbol{p}\lambda}(x)$ is the so-called Volkov solution of the Dirac equation [32,33],

$$\psi^{(+)}_{\boldsymbol{p}\lambda}(x) = \sqrt{\frac{m_{\rm e}c^2}{VE_{\boldsymbol{p}}}}\left(1 - \frac{e}{2k\cdot p}\not{A}\not{k}\right) u^{(+)}_{\boldsymbol{p}\lambda} e^{-iS^{(+)}_p(x)}, \tag{5}$$

with

$$S^{(+)}_p(x) = p\cdot x + \int_{-\infty}^{k\cdot x}\left[\frac{eA(\phi)\cdot p}{k\cdot p} - \frac{e^2A^2(\phi)}{2k\cdot p}\right]d\phi. \tag{6}$$

Moreover, $E_{\boldsymbol{p}} = cp^0$, $p = (p^0,\boldsymbol{p})$, $p\cdot p = m_{\rm e}^2c^2$, and $u^{(+)}_{\boldsymbol{p}\lambda}$ is the free-electron bispinor normalized such that

$$\bar{u}^{(+)}_{\boldsymbol{p}\lambda} u^{(+)}_{\boldsymbol{p}\lambda'} = \delta_{\lambda\lambda'}. \tag{7}$$

The four-vector potential $A(k\cdot x)$ in Eq. (5) represents an external electromagnetic radiation generated by lasers in the case when a transverse variation of the laser field in a focus is negligible. In this case, one can derive the exact solution to the Dirac equation coupled to the electromagnetic field [Eq. (5)], provided that $k\cdot A(k\cdot x) = 0$ and $k\cdot k = 0$.

In our further discussion, we shall adopt the Coulomb gauge for the radiation field which means that the four-vector $A(k\cdot x)$ has the vanishing zero component and that the electric and magnetic fields are equal to

$$\boldsymbol{\mathcal{E}}(k\cdot x) = -\partial_t \boldsymbol{A}(k\cdot x) = -ck^0\boldsymbol{A}'(k\cdot x), \tag{8}$$

$$\boldsymbol{\mathcal{B}}(k\cdot x) = \boldsymbol{\nabla}\times\boldsymbol{A}(k\cdot x) = -\boldsymbol{k}\times\boldsymbol{A}'(k\cdot x), \tag{9}$$

where "*prime*" means the derivative with respect to $k\cdot x$. Let us also remember that the electric field generated by lasers has to fulfill the following condition [34]:

$$\int_{-\infty}^{\infty} \boldsymbol{\mathcal{E}}(ck^0t - \boldsymbol{k}\cdot\boldsymbol{r})dt = 0, \tag{10}$$

which is followed by

$$\lim_{t\to-\infty} \boldsymbol{A}(ck^0t - \boldsymbol{k}\cdot\boldsymbol{r}) = \lim_{t\to\infty} \boldsymbol{A}(ck^0t - \boldsymbol{k}\cdot\boldsymbol{r}). \tag{11}$$

In the next sections, we shall consider two cases; when the vector potential $A(k\cdot x)$ describes a sequence of identical laser pulses (the so-called train of pulses, for which the plane wave is a particular realization) or a single laser pulse. Each of these situations requires a separate theoretical treatment.

A. Train of laser pulses

Let us assume that the duration of a single pulse within the field is $T_{\rm p}$. This means that the electromagnetic potential can be expanded as a Fourier series with the fundamental frequency $\omega = ck^0 = 2\pi/T_{\rm p}$,

$$A(k\cdot x) = \sum_{N=\pm1,\pm2,\ldots} A_N \exp(-iNk\cdot x). \tag{12}$$

Here, we do not account for the zero Fourier component since it can be eliminated by the gauge transformation of the vector potential. Moreover, in actual computations, we account only for a finite number of higher harmonics. Let us also remember that it is usually assumed that the laser field is adiabatically switched on in the remote past and switched off in the far future. Thus, the electron momentum present in Eq. (5) can be interpreted as the field-free asymptotic momentum of the

electron. Having this in mind, we consider the most general form of the laser field,

$$A(k\cdot x) = A_0[\varepsilon_1 f_1(k\cdot x) + \varepsilon_2 f_2(k\cdot x)], \tag{13}$$

in which two real four-vectors ε_i describe two linear polarizations of the laser field such that $\varepsilon_i^2 = -1$, $\varepsilon_1\cdot\varepsilon_2 = 0$ and $k\cdot\varepsilon_i = 0$. Moreover, $k = k^0(1,\boldsymbol{n})$ and the normalized to 1 vector $\boldsymbol{n}$ determines the direction of propagation of the laser beam. Let us note that in the case of a pulse train, the so-called shape functions $f_i(\phi)$ are periodic functions of ϕ with the period equal to 2π. They are, however, not periodic for the case of a single laser pulse, as will be discussed in the next section. Hence, the probability amplitude for the Compton process equals

$$\mathcal{A}\big(e^-_{\boldsymbol{p}_{\rm i}\lambda_{\rm i}} \longrightarrow e^-_{\boldsymbol{p}_{\rm f}\lambda_{\rm f}} + \gamma_{\boldsymbol{K}\sigma}\big) = i\sqrt{\frac{2\pi\alpha c(m_{\rm e}c^2)^2}{E_{\boldsymbol{p}_{\rm f}}E_{\boldsymbol{p}_{\rm i}}\omega_{\boldsymbol{K}}V^3}}\,\mathcal{A}, \tag{14}$$

where α is the fine-structure constant, $\alpha = e^2/(4\pi\varepsilon_0 c)$, and

$$\begin{aligned}\mathcal{A} = \int d^4x e^{-i(S^{(+)}_{p_{\rm i}}(x) - S^{(+)}_{p_{\rm f}}(x) - K\cdot x)} &\times \bar{u}^{(+)}_{\boldsymbol{p}_{\rm f}\lambda_{\rm f}}\left(1 - \mu\frac{m_{\rm e}c}{2p_{\rm f}\cdot k}[f_1(k\cdot x)\not{\varepsilon}_1\not{k} + f_2(k\cdot x)\not{\varepsilon}_2\not{k}]\right)\\ &\times \not{\varepsilon}^*_{\boldsymbol{K}\sigma}\left(1 + \mu\frac{m_{\rm e}c}{2p_{\rm i}\cdot k}[f_1(k\cdot x)\not{\varepsilon}_1\not{k} + f_2(k\cdot x)\not{\varepsilon}_2\not{k}]\right)u^{(+)}_{\boldsymbol{p}_{\rm i}\lambda_{\rm i}}.\end{aligned} \tag{15}$$

In the above equation we have introduced the important relativistically invariant parameter,

$$\mu = \frac{|eA_0|}{m_{\rm e}c}, \tag{16}$$

which measures the intensity of the laser field. After some algebraic manipulations, we find that a phase present in Eq. (15) equals

$$S^{(+)}_{p_{\rm i}}(x) - S^{(+)}_{p_{\rm f}}(x) - K\cdot x = (\bar{p}_{\rm i} - \bar{p}_{\rm f} - K)\cdot x + G(k\cdot x), \tag{17}$$

where the so-called dressed by the laser field momentum has been introduced,

$$\bar{p} = p + \frac{1}{2}(\mu m_{\rm e}c)^2\frac{\langle f_1^2\rangle + \langle f_2^2\rangle}{p\cdot k}k. \tag{18}$$

We have found also that

$$\begin{aligned}G(k\cdot x) = \int_0^{k\cdot x} d\phi\Big[&-\mu m_{\rm e}c\left(\frac{p_{\rm i}\cdot\varepsilon_1}{p_{\rm i}\cdot k} - \frac{p_{\rm f}\cdot\varepsilon_1}{p_{\rm f}\cdot k}\right)f_1(\phi)\\ &-\mu m_{\rm e}c\left(\frac{p_{\rm i}\cdot\varepsilon_2}{p_{\rm i}\cdot k} - \frac{p_{\rm f}\cdot\varepsilon_2}{p_{\rm f}\cdot k}\right)f_2(\phi)\\ &+\frac{1}{2}(\mu m_{\rm e}c)^2\left(\frac{1}{p_{\rm i}\cdot k} - \frac{1}{p_{\rm f}\cdot k}\right)\\ &\times\left(f_1^2(\phi) - \langle f_1^2\rangle + f_2^2(\phi) - \langle f_2^2\rangle\right)\Big].\end{aligned} \tag{19}$$

In the above equations, we understand that

$$\langle f\rangle = \frac{1}{T_{\rm p}}\int_0^{T_{\rm p}} dt f(ck^0t - \boldsymbol{k}\cdot\boldsymbol{r}) = \frac{1}{2\pi}\int_0^{2\pi} d\phi f(\phi). \tag{20}$$

Since for a train of laser pulses there is no zero Fourier component of shape functions, we have $\langle f_i\rangle = 0$. At this point, let us emphasize that this is not in general true for a single laser pulse.

The advantage of applying the decomposition (17) consists in the fact that $G(k\cdot x)$ in Eq. (19) is a periodic function of its argument $k\cdot x$. Hence, we can make the following Fourier expansion,

$$[f_1(k\cdot x)]^n[f_2(k\cdot x)]^m e^{-iG(k\cdot x)} = \sum_{N=-\infty}^{\infty} G_N^{(n,m)} e^{-{\rm i}Nk\cdot x}. \tag{21}$$

For a monochromatic plane-wave laser field, the Fourier coefficients $G_N^{(n,m)}$ can be expressed in terms of the generalized Bessel functions. For a general pulse, they are represented by a multiple sum over the product of many ordinary Bessel functions, and for this reason we do not present their explicit form (see, e.g., for a bichromatic laser field in the context of laser-induced pair creation [35]). Using the above series expansion we can now carry out the space-time integration in Eq. (15). This leads to

$$\mathcal{A} = \sum_N D_N \int d^4x e^{-i(\bar{p}_{\rm i} + Nk - \bar{p}_{\rm f} - K)\cdot x}, \tag{22}$$

where

$$\begin{aligned}D_N = \bar{u}^{(+)}_{\boldsymbol{p}_{\rm f}\lambda_{\rm f}}\not{\varepsilon}^*_{\boldsymbol{K}\sigma}u^{(+)}_{\boldsymbol{p}_{\rm i}\lambda_{\rm i}}G_N^{(0,0)} &+ \frac{1}{2}\mu m_{\rm e}c\Bigg[\left(\frac{1}{p_{\rm i}\cdot k}\bar{u}^{(+)}_{\boldsymbol{p}_{\rm f}\lambda_{\rm f}}\not{\varepsilon}^*_{\boldsymbol{K}\sigma}\not{\varepsilon}_1\not{k}u^{(+)}_{\boldsymbol{p}_{\rm i}\lambda_{\rm i}} - \frac{1}{p_{\rm f}\cdot k}\bar{u}^{(+)}_{\boldsymbol{p}_{\rm f}\lambda_{\rm f}}\not{\varepsilon}_1\not{k}\not{\varepsilon}^*_{\boldsymbol{K}\sigma}u^{(+)}_{\boldsymbol{p}_{\rm i}\lambda_{\rm i}}\right)G_N^{(1,0)}\\ &+\left(\frac{1}{p_{\rm i}\cdot k}\bar{u}^{(+)}_{\boldsymbol{p}_{\rm f}\lambda_{\rm f}}\not{\varepsilon}^*_{\boldsymbol{K}\sigma}\not{\varepsilon}_2\not{k}u^{(+)}_{\boldsymbol{p}_{\rm i}\lambda_{\rm i}} - \frac{1}{p_{\rm f}\cdot k}\bar{u}^{(+)}_{\boldsymbol{p}_{\rm f}\lambda_{\rm f}}\not{\varepsilon}_2\not{k}\not{\varepsilon}^*_{\boldsymbol{K}\sigma}u^{(+)}_{\boldsymbol{p}_{\rm i}\lambda_{\rm i}}\right)G_N^{(0,1)}\Bigg] - \frac{(\mu m_{\rm e}c)^2}{4(p_{\rm i}\cdot k)(p_{\rm f}\cdot k)}\Big[\bar{u}^{(+)}_{\boldsymbol{p}_{\rm f}\lambda_{\rm f}}\not{\varepsilon}_1\not{k}\not{\varepsilon}^*_{\boldsymbol{K}\sigma}\not{\varepsilon}_1\not{k}u^{(+)}_{\boldsymbol{p}_{\rm i}\lambda_{\rm i}}G_N^{(2,0)}\\ &+\bar{u}^{(+)}_{\boldsymbol{p}_{\rm f}\lambda_{\rm f}}\not{\varepsilon}_2\not{k}\not{\varepsilon}^*_{\boldsymbol{K}\sigma}\not{\varepsilon}_2\not{k}u^{(+)}_{\boldsymbol{p}_{\rm i}\lambda_{\rm i}}G_N^{(0,2)} + \left(\bar{u}^{(+)}_{\boldsymbol{p}_{\rm f}\lambda_{\rm f}}\not{\varepsilon}_1\not{k}\not{\varepsilon}^*_{\boldsymbol{K}\sigma}\not{\varepsilon}_2\not{k}u^{(+)}_{\boldsymbol{p}_{\rm i}\lambda_{\rm i}} + \bar{u}^{(+)}_{\boldsymbol{p}_{\rm f}\lambda_{\rm f}}\not{\varepsilon}_2\not{k}\not{\varepsilon}^*_{\boldsymbol{K}\sigma}\not{\varepsilon}_1\not{k}u^{(+)}_{\boldsymbol{p}_{\rm i}\lambda_{\rm i}}\right)G_N^{(1,1)}\Big].\end{aligned} \tag{23}$$

Performing now the integration in Eq. (22), which leads to the four-momenta conservation condition,

$$\bar{p}_{\rm i} + Nk - \bar{p}_{\rm f} - K = 0, \tag{24}$$

we arrive at the angular distribution of energy power of Compton photons that with polarization σ are emitted in the space direction $\boldsymbol{n}_{\boldsymbol{K}}$, provided that the initial electron has the momentum $\boldsymbol{p}_{\rm i}$ and the spin polarization $\lambda_{\rm i}$,

$$\frac{d^2P_{\rm C}^{(\rm t)}(\boldsymbol{n}_{\boldsymbol{K}}\sigma;\boldsymbol{p}_{\rm i}\lambda_{\rm i})}{d\Omega_{\boldsymbol{K}}} = \sum_N\sum_{\lambda_{\rm f}}\int d^3p_{\rm f}d\omega_{\boldsymbol{K}}\frac{\alpha(m_{\rm e}c^2)^2\omega_{\boldsymbol{K}}^2}{2\pi cE_{\boldsymbol{p}_{\rm i}}E_{\boldsymbol{p}_{\rm f}}}|D_N|^2\delta^{(4)}(\bar{p}_{\rm i} + Nk - \bar{p}_{\rm f} - K). \tag{25}$$

Due to the presence of the delta function, the remaining integrals can be performed exactly. Let us note first that since $K = K^0 n_{\boldsymbol{K}} = K^0(1,\boldsymbol{n}_{\boldsymbol{K}})$, the momentum conservation condition (24) leads to

$$K^0 = N\frac{k\cdot p_{\rm i}}{n_{\boldsymbol{K}}\cdot(\bar{p}_{\rm i}+Nk)}, \tag{26}$$

and

$$\bar{p}_{\rm f} = \bar{p}_{\rm i} + Nk - NK\frac{k\cdot p_{\rm i}}{K\cdot(\bar{p}_{\rm i}+Nk)}. \tag{27}$$

Hence, the final dressed electron momentum $\bar{p}_{\rm f}$ is independent of K^0, and

$$\int dK^0\delta^{(1)}\big(\bar{p}_{\rm i}^0 + Nk^0 - \bar{p}_{\rm f}^0 - K^0\big) = 1. \tag{28}$$

Moreover,

$$\int d^3p_{\rm f}\,\delta^{(3)}(\bar{\boldsymbol{p}}_{\rm i} + N\boldsymbol{k} - \bar{\boldsymbol{p}}_{\rm f} - \boldsymbol{K}) = \left|\frac{\partial\boldsymbol{p}_{\rm f}}{\partial\bar{\boldsymbol{p}}_{\rm f}}\right| = \frac{p_{\rm f}^0}{\bar{p}_{\rm f}^0}, \tag{29}$$

and finally,

$$\frac{d^2P_{\rm C}^{(\rm t)}(\boldsymbol{n}_{\boldsymbol{K}}\sigma;\boldsymbol{p}_{\rm i}\lambda_{\rm i})}{d\Omega_{\boldsymbol{K}}} = \sum_N\sum_{\lambda_{\rm f}}\frac{\alpha(m_{\rm e}c)^2\omega_{\boldsymbol{K}}^2}{2\pi p_{\rm i}^0\bar{p}_{\rm f}^0}|D_N|^2. \tag{30}$$

Multiplying the above equation by the duration of a single pulse $T_{\rm p}$, we obtain the energy distribution which is emitted in the direction $\boldsymbol{n}_{\boldsymbol{K}}$ with the polarization σ per pulse,

$$\frac{d^2E_{\rm C}^{(\rm t)}(\boldsymbol{n}_{\boldsymbol{K}}\sigma;\boldsymbol{p}_{\rm i}\lambda_{\rm i})}{d\Omega_{\boldsymbol{K}}} = T_{\rm p}\sum_N\sum_{\lambda_{\rm f}}\frac{\alpha(m_{\rm e}c)^2\omega_{\boldsymbol{K}}^2}{2\pi p_{\rm i}^0\bar{p}_{\rm f}^0}|D_N|^2. \tag{31}$$

For a monochromatic plane-wave laser field, being a particular realization of the laser pulse train, the integer N is interpreted as a net number of laser photons absorbed during the process. In a more general case of a multichromatic field, the quantity $N\hbar\omega$, where $\omega = ck^0$, is a net energy absorbed from the laser field. This interpretation allows one to define the angular and frequency distribution of energy emitted as Compton photons which, based on Eq. (31), is

$$\frac{d^2E_{{\rm C},N}^{(\rm t)}(\boldsymbol{n}_{\boldsymbol{K}}\sigma;\boldsymbol{p}_{\rm i}\lambda_{\rm i})}{d\Omega_{\boldsymbol{K}}} = T_{\rm p}\sum_{\lambda_{\rm f}}\frac{\alpha(m_{\rm e}c)^2\omega_{\boldsymbol{K}}^2}{2\pi p_{\rm i}^0\bar{p}_{\rm f}^0}|D_N|^2. \tag{32}$$

If we are not interested in polarization and spin effects, then we sum up over σ and average with respect to $\lambda_{\rm i}$,

$$\frac{d^2E_{{\rm C},N}^{(\rm t)}(\boldsymbol{n}_{\boldsymbol{K}};\boldsymbol{p}_{\rm i})}{d\Omega_{\boldsymbol{K}}} = \frac{1}{2}\sum_{\sigma=1,2}\sum_{\lambda_{\rm i}=\pm}\frac{d^2E_{{\rm C},N}^{(\rm t)}(\boldsymbol{n}_{\boldsymbol{K}}\sigma;\boldsymbol{p}_{\rm i}\lambda_{\rm i})}{d\Omega_{\boldsymbol{K}}}, \tag{33}$$

which symbolically can be written as

$$\frac{d^3E_{\rm C}^{(\rm t)}(\boldsymbol{n}_{\boldsymbol{K}};\boldsymbol{p}_{\rm i})}{dN{\rm d}\Omega_{\boldsymbol{K}}} = \frac{d^2E_{{\rm C},N}^{(\rm t)}(\boldsymbol{n}_{\boldsymbol{K}};\boldsymbol{p}_{\rm i})}{d\Omega_{\boldsymbol{K}}}, \tag{34}$$

and interpreted as the angular and frequency (since there is one-to-one correspondence between N and the Compton photon frequency $\omega_{\boldsymbol{K}}$) distribution of radiation energy generated during the process per one laser pulse.

B. Single laser pulse

In this section, we will formulate theory for the Compton process by an isolated laser pulse. Let a pulse last for a period $T_{\rm p}$. This introduces the fundamental frequency $\omega = 2\pi/T_{\rm p}$ and the laser field four-vector $k = k^0(1,\boldsymbol{n})$, where $\omega = ck^0$, with a direction of the laser pulse propagation given by the unit vector $\boldsymbol{n}$. Thus, the laser field potential is of the form (13), with the same meaning of the symbols as above. In order to interpret the momentum p in the Volkov solution (5) as the asymptotic momentum of the free electron (in both the remote past and the far future), we assume that

$$A(k\cdot x) = 0 \quad\text{for}\quad k\cdot x < 0 \quad\text{and}\quad k\cdot x > 2\pi. \tag{35}$$

Similar to the case of a laser pulse train, we expand the four-vector potential $A(k\cdot x)$ in the Fourier series. This time, however, in order to maintain the condition (35), a constant term in the Fourier expansion can appear. Such a term will be absent in the electric field (8), so that the obligatory conditions, (10) and (11), for the laser field can be satisfied. At this point let us stress that the existence of the zero Fourier component in (13) may have profound consequences. Basically, since it leads to a nonvanishing $\langle f_i\rangle$, a modified definition of the laser-dressed momentum must be introduced,

$$\bar{p} = p - \mu m_{\rm e}c\left(\frac{p\cdot\varepsilon_1}{p\cdot k}\langle f_1\rangle + \frac{p\cdot\varepsilon_2}{p\cdot k}\langle f_2\rangle\right)k + \frac{1}{2}(\mu m_{\rm e}c)^2\frac{\langle f_1^2\rangle + \langle f_2^2\rangle}{p\cdot k}k. \tag{36}$$

Since now $\bar{p}$ is polarization dependent one may expect, for instance, to observe asymmetries in angular distributions of the Compton photons. This will be discussed in detail in Sec. V.

Next, we have to reformulate the theory in such a way that it could effectively be used in numerical investigations. To this end let us go back to the space-time integral (15). It can be expressed in terms of integrals,

$$C^{(n,m)} = \int d^4x[f_1(k\cdot x)]^n[f_2(k\cdot x)]^m e^{-i[S_{p_{\rm i}}^{(+)}(x) - S_{p_{\rm f}}^{(+)}(x) - K\cdot x]}, \tag{37}$$

with $n,m = 0,1,2$. By passing to the light-cone variables (Appendix A) we see that the integral over x^- is limited to the finite region, $0 \leqslant x^- \leqslant 2\pi/k^0$, provided that n and m are not simultaneously equal to 0. Hence, in order to determine numerically $C^{(0,0)}$ we have to transform this integral to a more suitable form; this is done by applying the Boca-Florescu transformation presented in Appendix B. We have the following correspondences:

$$Q = p_{\rm i} - p_{\rm f} - K, \tag{38}$$

and

$$h(\phi) = a_1 f_1(\phi) + a_2 f_2(\phi) + b\big[f_1^2(\phi) + f_2^2(\phi)\big], \tag{39}$$

with

$$a_1 = -\mu m_e c\left(\frac{p_i\cdot\varepsilon_1}{p_i\cdot k} - \frac{p_f\cdot\varepsilon_1}{p_f\cdot k}\right) = -Q^0\tilde{a}_1/k^0,$$
$$a_2 = -\mu m_e c\left(\frac{p_i\cdot\varepsilon_2}{p_i\cdot k} - \frac{p_f\cdot\varepsilon_2}{p_f\cdot k}\right) = -Q^0\tilde{a}_2/k^0, \quad (40)$$
$$b = \frac{1}{2}(\mu m_e c)^2\left(\frac{1}{p_i\cdot k} - \frac{1}{p_f\cdot k}\right) = -Q^0\tilde{b}/k^0,$$

which also defines parameters $\tilde{a}_i$ and $\tilde{b}$, provided that $Q^0 \neq 0$. We shall demonstrate below that this condition is always fulfilled [see Eq. (49) below]. Finally, applying Eq. (B11) we arrive at

$$C^{(0,0)} = \int d^4x\{\tilde{a}_1 f_1(k\cdot x) + \tilde{a}_2 f_2(k\cdot x) + \tilde{b}[f_1^2(k\cdot x) + f_2^2(k\cdot x)]\}e^{-i[S_{p_i}^{(+)}(x) - S_{p_f}^{(+)}(x) - K\cdot x]}. \quad (41)$$

The next steps basically follow the procedure of Sec. II A. We make the decomposition, similar to Eq. (17),

$$S_{p_i}^{(+)}(x) - S_{p_f}^{(+)}(x) - K\cdot x = (\bar{p}_i - \bar{p}_f - K)\cdot x + G(k\cdot x), \quad (42)$$

with the dressed momenta defined by Eq. (36), and

$$G(k\cdot x) = \int_0^{k\cdot x} d\phi\Big[-\mu m_e c\left(\frac{p_i\cdot\varepsilon_1}{p_i\cdot k} - \frac{p_f\cdot\varepsilon_1}{p_f\cdot k}\right) \times (f_1(\phi) - \langle f_1\rangle) - \mu m_e c\left(\frac{p_i\cdot\varepsilon_2}{p_i\cdot k} - \frac{p_f\cdot\varepsilon_2}{p_f\cdot k}\right) \times (f_2(\phi) - \langle f_2\rangle) + \frac{1}{2}(\mu m_e c)^2\left(\frac{1}{p_i\cdot k} - \frac{1}{p_f\cdot k}\right) \times \left(f_1^2(\phi) - \langle f_1^2\rangle + f_2^2(\phi) - \langle f_2^2\rangle\right)\Big]. \quad (43)$$

Now, after applying the Fourier decompositions (21), we obtain D_N similar to (23) with the only replacement,

$$G_N^{(0,0)} \to \tilde{a}_1 G_N^{(1,0)} + \tilde{a}_2 G_N^{(0,1)} + \tilde{b}[G_N^{(2,0)} + G_N^{(0,2)}], \quad (44)$$

which follows from the application of the Boca-Florescu transformation with respect to Eq. (41).

Performing the space-time integration in Eq. (15) and keeping in mind that $0 \leqslant x^- \leqslant 2\pi/k^0$, we arrive at

$$\mathcal{A} = \sum_N (2\pi)^3\delta^{(1)}(P_N^-)\delta^{(2)}(\boldsymbol{P}_N^\perp)D_N\frac{1 - e^{-2\pi i P_N^+/k^0}}{iP_N^+}, \quad (45)$$

where

$$P_N = \bar{p}_i + Nk - \bar{p}_f - K. \quad (46)$$

In order to solve the momentum conservation conditions imposed by the three delta functions, let us introduce the four-vector $w = p_i - K$, so that

$$p_f^0 = p_f^\parallel + w^-, \quad \boldsymbol{p}_f^\perp = \boldsymbol{w}^\perp. \quad (47)$$

Since the electron mass is different from zero, it follows from the first equation that $w^- > 0$, and

$$p_f^\parallel = \frac{(m_e c)^2 - (w^-)^2 + \boldsymbol{w}_\perp^2}{2w^-} = \frac{K\cdot p_i}{w^-} + w^\parallel, \quad (48)$$

which means that

$$Q^0 = p_i^0 - p_f^0 - K^0 = p_i^\parallel - p_f^\parallel - K^\parallel = -\frac{p_i\cdot K}{w^-} < 0. \quad (49)$$

This is exactly the applicability condition for the Boca-Florescu transformation (B11).

Since $\boldsymbol{P}_N^\perp$ and P_N^- do not depend explicitly on N, and

$$\int d^3p_f\,\delta^{(1)}(P_N^-)\delta^{(2)}(\boldsymbol{P}_N^\perp) = \frac{k^0 p_f^0}{k\cdot p_f}, \quad (50)$$

we obtain the differential distribution of energy,

$$\frac{d^3E_C^{(p)}(\boldsymbol{K}\sigma;\boldsymbol{p}_i\lambda_i)}{d\omega_{\boldsymbol{K}}d^2\Omega_{\boldsymbol{K}}} = \sum_{\lambda_f}\frac{\alpha(m_e c)^2k^0(K^0)^2}{(2\pi)^2p_i^0(k\cdot p_f)} \times\left|\sum_N D_N\frac{1 - e^{-2\pi i P_N^0/k^0}}{P_N^0}\right|^2, \quad (51)$$

emitted as Compton photons by a single pulse, or if we are not interested in polarization effects,

$$\frac{d^3E_C^{(p)}(\boldsymbol{K};\boldsymbol{p}_i)}{d\omega_{\boldsymbol{K}}d^2\Omega_{\boldsymbol{K}}} = \frac{1}{2}\sum_{\sigma=1,2}\sum_{\lambda_i=\pm}\frac{d^3E_C^{(p)}(\boldsymbol{K}\sigma;\boldsymbol{p}_i\lambda_i)}{d\omega_{\boldsymbol{K}}d^2\Omega_{\boldsymbol{K}}}. \quad (52)$$

Here, the question arises: how to define the energy distribution of Compton photons scattered by a single laser pulse so it is meaningful to compare it with the distribution (34). To answer this question let us go back to Eq. (45) and note that for a very long pulse the maximum of $|\mathcal{A}|^2$ is achieved for $P_N^+ = P_N^0 = 0$. This allows us to define the effective energy $N_{\rm eff}\hbar ck^0$ absorbed from a laser pulse as compared to the energy $N\hbar ck^0$ absorbed from a train of laser pulses such that $P_{N_{\rm eff}}^0 = 0$, that is,

$$N_{\rm eff} = \frac{K^0 + \bar{p}_f^0 - \bar{p}_i^0}{k^0} = cT_p\frac{K^0 + \bar{p}_f^0 - \bar{p}_i^0}{2\pi}. \quad (53)$$

Hence, we can define an analog of (34) for an isolated laser pulse,

$$\frac{d^3E_C^{(p)}(\boldsymbol{K};\boldsymbol{p}_i)}{dN_{\rm eff}d^2\Omega_{\boldsymbol{K}}} = \frac{d\omega_{\boldsymbol{K}}}{dN_{\rm eff}}\frac{d^3E_C^{(p)}(\boldsymbol{K};\boldsymbol{p}_i)}{d\omega_{\boldsymbol{K}}d^2\Omega_{\boldsymbol{K}}}. \quad (54)$$

We do not present here the explicit form for the derivative $d\omega_{\boldsymbol{K}}/dN_{\rm eff}$ which is rather lengthy and can be determined numerically in a more efficient way. The aim of this paper, among others, is to discuss for how long laser pulses two formulas given by Eqs. (34) and (54) provide similar results.

III. SHAPE FUNCTIONS

In our further investigations, we shall consider linearly polarized laser pulses which propagate in the z direction ($\boldsymbol{n} = \boldsymbol{e}_z$), with a polarization along the x axis ($\boldsymbol{\varepsilon}_1 = \boldsymbol{e}_x$). This means that $f_2(\phi) = 0$, and so we shall denote the first shape function $f_1(\phi)$ simply as $f(\phi)$. This function has to be chosen such that the electric field satisfies the condition (10). Moreover, we shall assume that the laser pulse lasts for a finite time T_p. This excludes commonly used shape functions with envelops proportional to functions gradually decreasing in the remote past and the far future, like, for instance, the Gaussian

function or some rational combinations of the hyperbolic functions [20–23,25] (we also exclude rectangular pulses as unphysical). This will allow us to define without an ambiguity the number of oscillations within the pulse (as opposed, for instance, to Ref. [20]). There are many possibilities for choosing such functions, but for the purpose of this publication we consider the following one-parameter shape function,

$$f'(k\cdot x) = N_{\rm A}\sin^2\left(\frac{k_{\rm L}\cdot x}{2N_{\rm osc}}\right)\sin(k_{\rm L}\cdot x) = N_{\rm A}\sin^2\left(\frac{k\cdot x}{2}\right)\sin(N_{\rm osc}k\cdot x), \qquad (55)$$

for $0 \leqslant k_{\rm L}\cdot x \leqslant 2\pi N_{\rm osc}$, and 0 otherwise. The pulse duration equals $T_{\rm p} = 2\pi N_{\rm osc}/\omega_{\rm L}$, hence $k_{\rm L} = (\omega_{\rm L}/c)(1,\boldsymbol{n}) = N_{\rm osc}k$. Moreover, $\omega_{\rm L}$ is the central frequency of the laser pulse.

Let us mention that the shape function (55) determines both the electric and magnetic fields of the laser pulse, Eqs. (8) and (9), respectively. Hence, the shape function for the four-vector potential equals

$$f(k\cdot x) = \int_0^{k\cdot x} d\phi f'(\phi), \qquad (56)$$

and vanishes for $k\cdot x < 0$ and $k\cdot x > 2\pi$. In Eq. (55), the free parameter, $N_{\rm osc} = 1,2,\ldots,$ determines the number of oscillations within the pulse. The normalization constant $N_{\rm A}$ is defined such that

$$\langle (f-f_0)^2\rangle = \frac{1}{2\pi}\int_0^{2\pi}(f(\phi)-f_0)^2 d\phi = \frac{1}{2}, \qquad (57)$$

in order to establish the connection with the monochromatic plane-wave approximation. In the above equation, f_0 is the constant term in the Fourier expansion of $f(\phi)$. Both shape functions, $f'(k\cdot x)$ and $f(k\cdot x)$, for some small $N_{\rm osc}$ are presented in Fig. 1. As one can anticipate from this figure, for the given values of $N_{\rm osc}$, $\langle f\rangle \neq 0$. However, with increasing the number of laser field oscillations $\langle f\rangle$ starts to deteriorate, and finally goes to 0. Therefore, we expect that for sufficiently long laser pulses the energy spectrum of Compton photons will approach the one for a train of laser pulses. This will be illustrated in the next section.

We want to emphasize that the aforementioned discussion relates to a single laser pulse. For a train of pulses, the only difference is that the shape function for the electric and magnetic fields, given by Eq. (55), is repeated for all times. This means that for the pulse train, $f'(k\cdot x)$ and $f(k\cdot x)$ are periodic functions of their argument, with vanishing zero Fourier components.

IV. FREQUENCY DISTRIBUTIONS

We start with discussing the frequency distribution of Compton radiation for a given $\boldsymbol{n_K}$ and for the case when electrons are initially at rest. For the laser field we choose the one generated by the Ti:sapphire laser with central frequency $\omega_{\rm L}$ such that $\hbar\omega_{\rm L} = 1.5$ eV $\approx 3\times 10^{-6} m_{\rm e}c^2$ (this corresponds approximately to wavelength 800 nm). Such a choice is motivated by the fact that presently these are the most powerful lasers generating electromagnetic radiation in the visible part of the spectrum. For very long laser pulses, the parameter

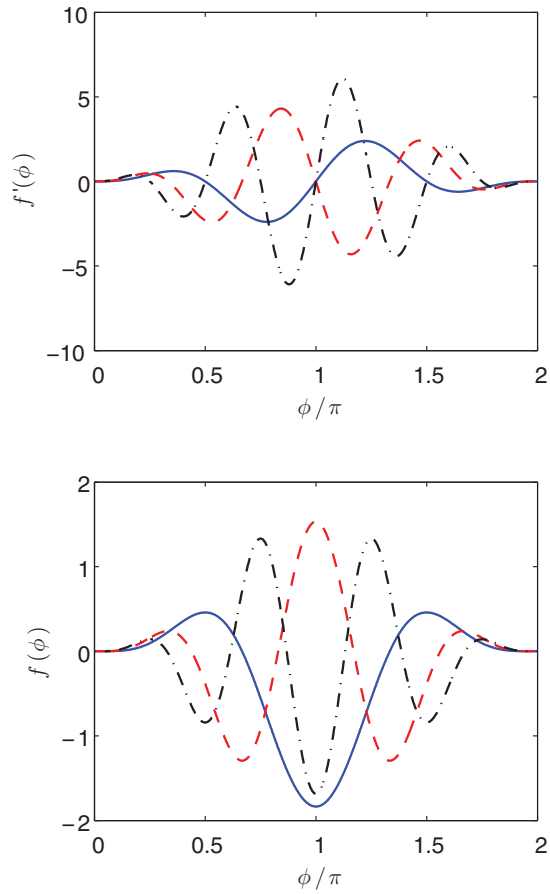

FIG. 1. (Color online) Laser field shape functions [defined by Eqs. (55) and (56)] normalized according to Eq. (57). Each curve relates to a different number of laser field oscillations, namely, $N_{\rm osc} = 2$ (solid blue line), $N_{\rm osc} = 3$ (dashed red line), and $N_{\rm osc} = 4$ (dash-dotted black line).

μ introduced in (16) equals 1 for the laser field intensity of the order of 10^{18} W/cm^2. It is instructive to realize that nowadays intensities of the order of $(10^{20}$–$10^{22})$ W/cm^2 are available experimentally [36], and those correspond roughly to $\mu \approx 7$–70.

In Fig. 2, we compare energy distributions of Compton photons scattered either by a single laser pulse, Eq. (54), by a train of such pulses, Eq. (34), and by a plane laser wave (which, in fact, is a train of pulses with a constant envelope) for the case when $\mu = 1$ and $N_{\rm osc} = 16$. We observe here a perfect agreement of the first two approaches and a failure of the monochromatic wave approximation. This agreement is also attained for much larger Compton frequencies provided that the spectra are plotted as functions of energy absorbed from the laser field (i.e., $N_{\rm eff}$ for an isolated laser pulse and N for a train of pulses); see the lower panel of Fig. 3. On the contrary, when the frequency dependence of emitted photons is investigated, a shift of energy spectra is observed (see the upper panel of Fig. 3). The shift is caused by a different dressing of the initial and final electron momenta for these two cases, which we have discussed above. As expected, for longer pulses this discrepancy gradually disappears since the constant term in the Fourier expansion of the electromagnetic potential for a single pulse becomes gradually smaller; this

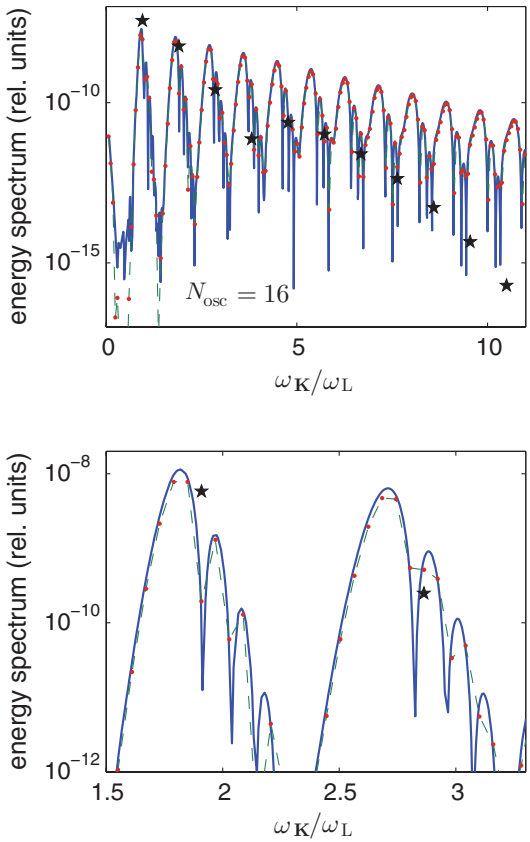

FIG. 2. (Color online) Energy spectra, Eqs. (34) and (54), for Compton photons emitted in the direction $\boldsymbol{n}_{\boldsymbol{K}}$ determined by the polar and azimuth angles $\theta_{\boldsymbol{K}} = 0.2$ and $\varphi_{\boldsymbol{K}} = 0$ (in radians). The initial electron is at rest and the laser photon frequency is such that $\hbar\omega_{\rm L} = 3 \times 10^{-6} m_{\rm e} c^2$. The intensity of the laser beam is determined by $\mu = 1$. The solid (blue) line corresponds to scattering by a single laser pulse, Eq. (54), the dashed (green) line to scattering by a train of pulses, Eq. (34), whereas the red bullets indicate the Compton photon frequencies, $\omega_{\boldsymbol{K}} = cK^0$ in Eq. (26), for integer N. The black pentagrams represent the energy spectrum (34) for a plane wave, when the shape function in Eq. (55) is proportional to $\sin(k_{\rm L} \cdot x)$. In all cases $N_{\rm osc} = 16$. The lower panel shows the enlarged part of the upper one in order to prove a very good agreement between the results obtained for a single pulse and a train of such pulses.

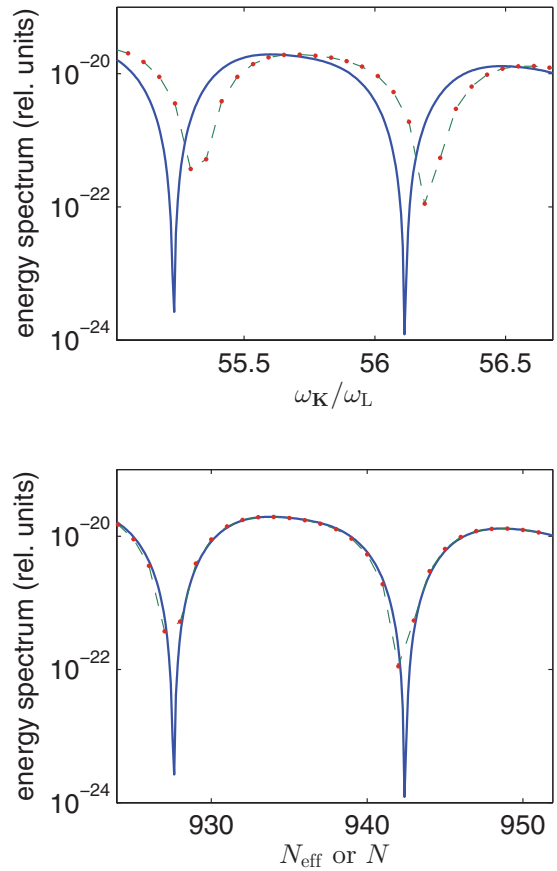

FIG. 3. (Color online) The same as in Fig. 2 but for larger frequencies (upper panel). In the upper panel, we clearly see the "blue-shift" of the spectrum for Compton photons scattered by a train of pulses, as compared to those scattered by an individual pulse. This shift is absent, however, when the spectra are shown as functions of $N_{\rm eff}$ or N (lower panel).

is confirmed by our results for even larger $N_{\rm osc}$ which we, however, do not present here. Instead, in Fig. 4 we show frequency distributions of emitted photons for extremely short laser pulses such that there is either two or even one oscillation within the pulse ($N_{\rm osc} = 2$ or 1, respectively). In both these cases, a significant disagreement of frequency distributions of Compton radiation for an individual pulse and a laser pulse train is observed, in addition to a pronounced discrepancy with the results obtained using the monochromatic plane-wave approximation. We confirm therefore that for ultrashort laser pulses available these days, a precise theoretical treatment of their temporal properties is indeed necessary.

It is worth noting the existence of regular side lobes in energy spectra of Compton photons, as shown in Fig. 2. Namely, apart from a dominating peak in the spectrum there are also subpeaks located asymmetrically on its right-hand side (i.e., for larger frequencies). The exactly same structure has been already observed and interpreted as the interference phenomenon in Ref. [21] (see also references therein).

In closing this section, let us comment on the momentum dressing in strong-field QED processes. In the case of a monochromatic laser field, such a dressing is gained when separating the classical action $S_p^{(+)}(x)$ [Eq. (6)] into oscillatory and linear parts. A similar approach has been proposed here, even though for finite laser pulses the respective periodicity of a four-vector potential is lost. The reason that we have introduced it anyway is that the concept of the momentum dressing allows one to define a convenient method for performing numerical calculations. In addition, a perfect agreement between the results for a single laser pulse and a laser pulse train observed in the lower panel of Fig. 3 indicates that the concept of quasimomenta is still valid for a 16-cycle laser pulse such that $\mu = 1$. As we have checked this for the same pulse duration but for stronger laser fields (larger μ), this agreement starts to deteriorate and the concept of momenta dressing breaks down eventually. This may have profound consequences, particularly when analyzing the laser-induced pair creation process, as it has been pointed out in Ref. [37].

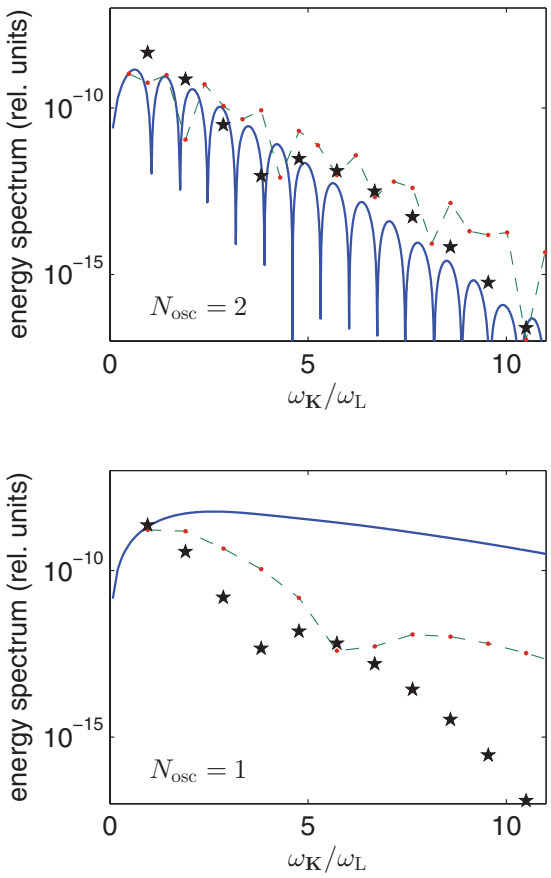

FIG. 4. (Color online) The same as in Fig. 2 but for very short pulses with $N_{\rm osc} = 2$ (upper panel) and $N_{\rm osc} = 1$ (lower panel). Let us note that pentagrams, representing the results for the monochromatic plane wave, in both these panels and in Fig. 2 provide the same results up to multiplication by the number of oscillations $N_{\rm osc}$.

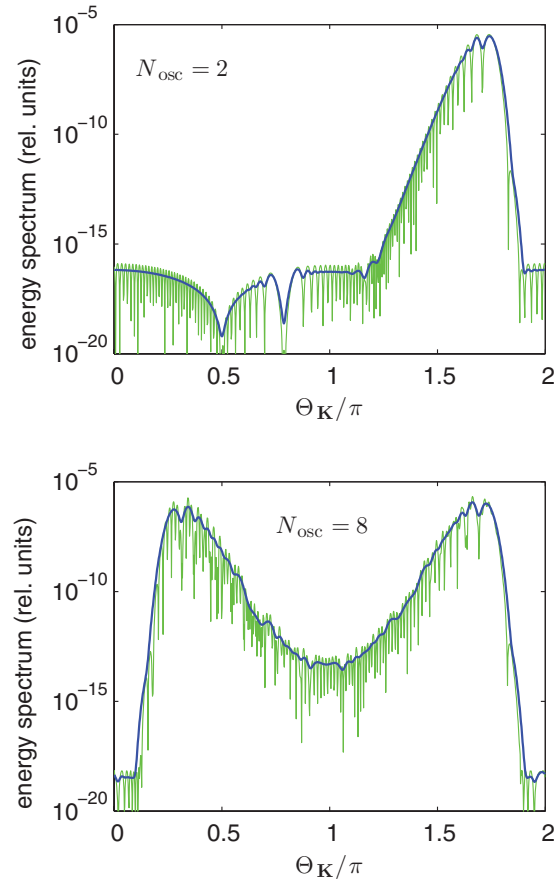

FIG. 5. (Color online) Angular distributions of the Compton radiation energy (green lines), Eq. (54), as functions of the angle $\Theta_{\boldsymbol{K}}$ in the plane spanned by the laser field propagation direction and the polarization vector (i.e., in the xz plane) for an ultrashort ($N_{\rm osc} = 2$, upper panel) and a relatively long ($N_{\rm osc} = 8$, lower panel) laser pulses. The laser field central frequency $\omega_{\rm L}$ is such that $\hbar\omega_{\rm L} = 3 \times 10^{-4} m_{\rm e}c^2$ whereas $\mu = 1$. The initial electron is at rest and the Compton photon energy equals $\hbar\omega_{\boldsymbol{K}} = 10^{-2} m_{\rm e}c^2$. The smooth blue lines represent the averaged distributions, as described by Eq. (60).

V. ANGULAR DISTRIBUTIONS

When discussing the angular distributions of Compton photons, it is more convenient to introduce a polar angle $\Theta_{\boldsymbol{K}}$ such that it is equal to $\theta_{\boldsymbol{K}}$ for $0 \leqslant \varphi_{\boldsymbol{K}} \leqslant \pi$, and $\Theta_{\boldsymbol{K}} = 2\pi - \theta_{\boldsymbol{K}}$ for the azimuthal angle $\varphi_{\boldsymbol{K}} + \pi$. With this definition, the distribution (54) is a periodic function of $\Theta_{\boldsymbol{K}}$. Usually, the angular distribution of the Compton radiation is a very rapidly changing function of $\Theta_{\boldsymbol{K}}$ for a given $\varphi_{\boldsymbol{K}}$. These changes cannot be observed experimentally because of the finite angular resolution of detectors. In order to account for this fact we have to average the spectrum (54) with some function, the so-called window function, concentrated around a given value of the polar angle $\Theta_{\boldsymbol{K}}$. Let us choose the window function as

$$W_\beta(\theta) = N_{\rm W}\left(\frac{1+\cos\theta}{2}\right)^\beta, \tag{58}$$

with $\beta > 0$, which is normalized such that

$$\int_0^{2\pi} d\theta\, W_\beta(\theta) = 1. \tag{59}$$

The parameter β defines the half-width of this function equal to the angular resolution of the detector. Let us assume that the angular resolution of a detector is roughly 0.02π radians, which is achieved if $\beta = 2048$. Then, the average of a periodic function $g(\theta)$ with the period 2π is defined as

$$\langle g\rangle_{W_\beta}(\Theta_{\boldsymbol{K}}) = \int_0^{2\pi} d\theta\, W_\beta(\Theta_{\boldsymbol{K}} - \theta) g(\theta). \tag{60}$$

This integration can be efficiently carried out by applying the fast Fourier transform. In our analysis, $g(\theta)$ is the differential energy distribution (54) for a given $\omega_{\boldsymbol{K}}$ and for a given azimuthal angle $\varphi_{\boldsymbol{K}}$.

In Fig. 5, we show angular distributions of the Compton radiation energy (green lines) which is emitted during electron scattering by a single laser pulse. While the upper panel shows the results for an ultrashort laser pulse with $N_{\rm osc} = 2$, the lower panel is for a relatively long laser pulse such that $N_{\rm osc} = 8$. In both cases, the central laser frequency is such that $\hbar\omega_{\rm L} = 3 \times 10^{-4} m_{\rm e}c^2$, and μ equals 1. As before, we assume that initially the colliding electron is at rest. The presented distributions are for a fixed energy of Compton photons such that $\hbar\omega_{\boldsymbol{K}} = 10^{-2} m_{\rm e}c^2$ and for $\varphi_{\boldsymbol{K}} = 0$. As was anticipated above, we observe very rapid oscillations of angular distributions, and so we plot also their average (60)

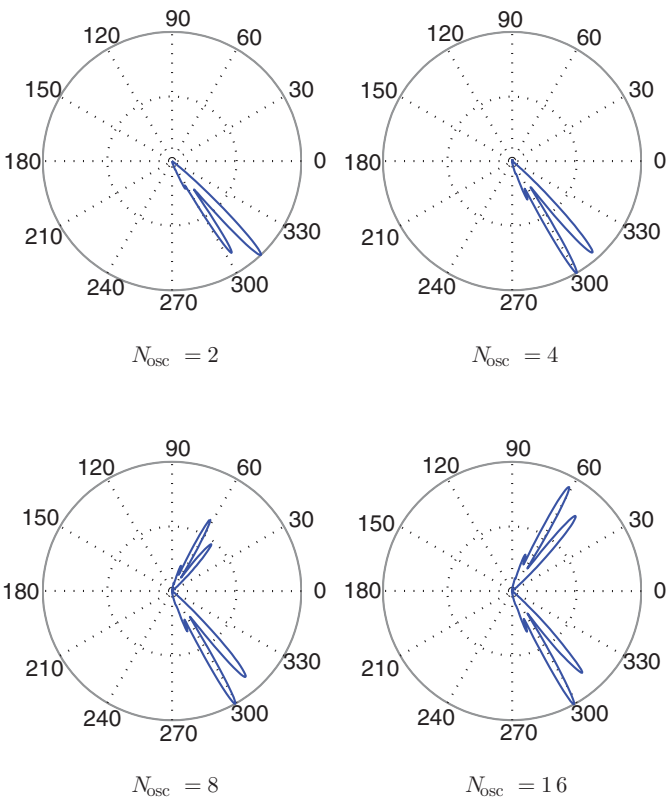

FIG. 6. (Color online) Polar plots of the (normalized to 1 and window-averaged) Compton photon energy distribution, Eq. (60), as functions of $\Theta_{\boldsymbol{K}}$ for different-cycle laser pulses with $N_{\rm osc} = 2,4,8$, and 16, as indicated under the plots. The other parameters are exactly the same as in Fig. 5.

which is represented by a blue line. For a two-cycle laser pulse, a strong asymmetry in angular distributions (54) and (60) is observed, which is the consequence of asymmetry of the shape function $f(\phi)$ with respect to the change of the polarization vector direction $\boldsymbol{\varepsilon}_1 \to -\boldsymbol{\varepsilon}_1$. Let us note that in the current case, the shape function of the electric field $f'(\phi)$ does not possess such an asymmetry. This indicates that symmetry properties of the electromagnetic potential (*not* the electric field) are responsible for symmetries of energy angular distributions of Compton photons. In Fig. 6, we present only window-averaged angular distributions (60) for laser pulses of different duration, namely, $N_{\rm osc} = 2,4,8$, and 16, and for the same parameters as in Fig. 5. Once again, we see that the angular asymmetry of those distributions, dominant for very short laser pulses, gradually disappears with increasing the number of laser field oscillations $N_{\rm osc}$. For $N_{\rm osc} = 16$, the angular distribution is roughly symmetric. We would like also to note that the corresponding distributions for Compton scattering by positrons are similar to Figs. 5 and 6, however, they are mirrored with respect to $\Theta_{\boldsymbol{K}} = \pi$.

Let us emphasize that all the results presented here relate to the case when an initial electron is at rest. In experiments, however, we deal with a situation when incident electrons move with very high kinetic energies; in the SLAC experiment reaching almost 50 GeV that corresponds to the Lorentz factor γ of the order of 10^5 [30,31]. In Refs. [30,31], these energetic electrons were colliding with a counterpropagating

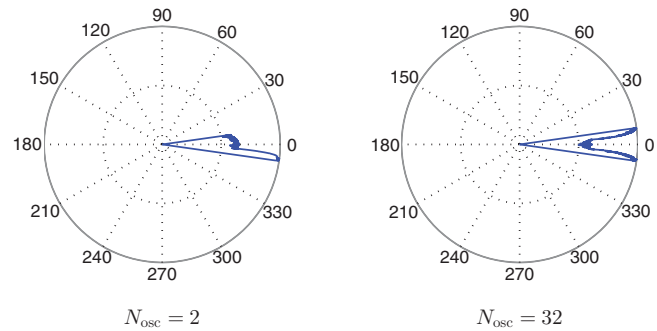

FIG. 7. (Color online) Polar plots of the normalized to one Compton radiation energy distribution (54) ($\hbar\omega_{\boldsymbol{K}} = 100 m_{\rm e}c^2$) as a function of $\Theta_{\boldsymbol{K}}$ for two- and 32-cycle laser pulses (left and right panels, respectively). Here, $\hbar\omega_{\rm L} = m_{\rm e}c^2$ (in the electron rest frame) and $\mu = 10$. For visual purposes, the rates have been raised to power 0.01.

laser beam to produce highly energetic radiation. We would like to emphasize that the calculations performed in this paper remain valid in the rest frame of the electron from the countermoving beam, if we scale the fundamental frequency of the laser field by roughly a factor of 2γ. This means that for a relativistic electron that moves with a large Lorentz factor γ and collides, for instance, with a Ti:sapphire laser field, the Doppler upshifted frequency of the laser field in the electron rest frame can reach $m_{\rm e}c^2$. For this reason, in Fig. 7 we present angular distributions of the Compton radiation for the case when in the electron rest frame the laser field central frequency is such that $\hbar\omega_{\rm L} = m_{\rm e}c^2$, and also $\mu = 10$. These distributions are for the Compton photons of energy $\hbar\omega_{\boldsymbol{K}} = 100 m_{\rm e}c^2$ (in the chosen reference frame) and they have been normalized to 1. Let us note that the probability rates of pair creation in the forward direction are significantly smaller (by roughly 20 orders of magnitude) than the offside lobes in angular distributions. For visual purposes, however, we have raised the data to power 0.01 so even small details of the spectra become visible. While in the right panel of Fig. 7 the results for a 32-cycle laser pulse are presented, in the left panel we show the results for a much shorter pulse which contains only two oscillations of the laser field. Even for much stronger fields than considered previously, we observe a very clear asymmetry in angular distributions of Compton photons for very short laser pulses. As before, this asymmetry is absent for long pulse durations. We would also like to point out that the angular distributions shown in Fig. 7 have not been averaged according to the prescription defined by Eq. (60). As one can observe for the given parameters, there is a small angular window within which the Compton photons are emitted. In general, it follows from $\delta^{(1)}(P_N^-)$ that is present in Eq. (45), that $p_{\rm i}^0 - p_{\rm i}^{\parallel} > K^0 - K^{\parallel}$ which imposes the limits on the scattering angle of Compton photons. In particular, in the electron rest frame this condition can be rewritten in a simple form,

$$\cos\Theta_{\boldsymbol{K}} > 1 - m_{\rm e}c^2/\omega_{\boldsymbol{K}}. \tag{61}$$

Hence, we find that for the parameters specified in Fig. 7 ($\hbar\omega_{\boldsymbol{K}} = 100 m_{\rm e}c^2$), the Compton photons are emitted in a cone

such that $|\Theta_{\boldsymbol{K}}| < \sqrt{2}/10$ radians. This agrees well with our numerical results.

VI. CONCLUSIONS

In this paper, the nonlinear Compton scattering of an intense laser beam by an electron has been considered. We have modeled the incident laser beam as a finite-length plane-wave-fronted laser pulse or a sequence of such pulses. For both cases, the frequency and angular distributions of energy emitted as Compton photons have been unambiguously defined such that a comparison between these two cases became meaningful. The theory of nonlinear Compton scattering that has been developed here accounts for, in principle, arbitrary laser pulses (i.e., arbitrary pulse shapes, pulse durations, etc.) which are used nowadays in experiments.

Here, we have envisaged the case when the initial electron is at rest and it is stroked by an intense laser beam. Comparing situations when the laser beam is represented by an individual laser pulse and by a train of such pulses we recognized that for pulses which include several oscillations of the laser field, both approaches lead to the seemingly same results for Compton radiation spectra. This agreement deteriorates, however, with decreasing duration of the incident pulse, and particularly for very-few-cycle pulses a detailed treatment of their spectral characteristic becomes important. A sensitivity of angular distributions of emitted photons to the incoming pulse duration was also investigated. We found that for ultrashort laser pulses the respective angular distributions show asymmetries which are due to asymmetries of the vector potential defining the incident laser beam. Those asymmetries disappear, however, for very long pulse durations.

ACKNOWLEDGMENTS

This work is supported by the Polish National Science Center (NCN) under Grant No. 2011/01/B/ST2/00381.

APPENDIX A: LIGHT-CONE COORDINATES

Throughout the paper, we apply the following definitions and notations for the light-cone coordinates. If the space direction is determined by a normalized to 1 space vector $\boldsymbol{n}$, then for an arbitrary four-vector a we introduce the light-cone coordinates such that

$$a^{\parallel} = \boldsymbol{n}\cdot\boldsymbol{a}, \quad a^{-} = a^{0} - a^{\parallel}, \quad a^{+} = \frac{a^{0}+a^{\parallel}}{2}, \qquad \boldsymbol{a}^{\perp} = \boldsymbol{a} - a^{\parallel}\boldsymbol{n}. \tag{A1}$$

With this definition,

$$a\cdot b = a^{0}b^{0} - \boldsymbol{a}\cdot\boldsymbol{b} = a^{-}b^{+} + a^{+}b^{-} - \boldsymbol{a}^{\perp}\cdot\boldsymbol{b}^{\perp}, \tag{A2}$$

and

$$d^{4}x = dx^{-}dx^{+}d^{2}\boldsymbol{x}^{\perp}. \tag{A3}$$

APPENDIX B: BOCA-FLORESCU TRANSFORMATION

Let $h(\phi)$ be a real and integrable function which does not vanish only within a finite interval, $\Phi_0 \leqslant \phi \leqslant \Phi$. We define also the integral,

$$H(\phi) = \int_{-\infty}^{\phi} du\, h(u). \tag{B1}$$

Let us note that $H(\phi)$ is 0 when $\phi < \Phi_0$, it is a constant if $\phi > \Phi$ [we shall further denote this constant as $H(\Phi) = \int_{\Phi_0}^{\Phi} du\, h(u)$], and rather than that it can have any value. We consider the integral,

$$C = \int d^{4}x\, e^{-iH(k\cdot x) - iQ\cdot x}, \tag{B2}$$

in which Q is an arbitrary four-vector and k satisfies the zero-mass on-shell relation, $k\cdot k = 0$. Let us assume that $k = k^{0}(1,\boldsymbol{n})$, where $\boldsymbol{n}^{2} = 1$ and $k^{0} > 0$. Hence, using the light-cone variables introduced in Appendix A, we obtain

$$C = (2\pi)^{3}\delta^{(1)}(Q^{-})\delta^{(2)}(\boldsymbol{Q}^{\perp})I(k^{0},Q^{+}), \tag{B3}$$

where

$$I(k^{0},Q^{+}) = \int dx^{-} e^{-i[H(k^{0}x^{-}) + Q^{+}x^{-}]}. \tag{B4}$$

Next, we regularize this integral similar to a regularization introduced in Ref. [20],

$$I_{\varepsilon}(k^{0},Q^{+}) = \int dx^{-} e^{-i[H(k^{0}x^{-}) + Q^{+}x^{-}] - \varepsilon|x^{-}|}, \tag{B5}$$

so that it becomes absolutely convergent. Here, it is understood that $\varepsilon > 0$. By noting that

$$\int dx^{-}[-i(k^{0}h(k^{0}x^{-}) + Q^{+}) - \varepsilon\,\mathrm{sgn}(x^{-})] \times e^{-i[H(k^{0}x^{-}) + Q^{+}x^{-}] - \varepsilon|x^{-}|} = e^{-i[H(k^{0}x^{-}) + Q^{+}x^{-}] - \varepsilon|x^{-}|}\Big|_{-\infty}^{+\infty} = 0, \tag{B6}$$

where $\mathrm{sgn}(x^{-})$ is the sign function, we arrive at

$$iQ_{+}I_{\varepsilon}(k^{0},Q_{+}) = I_{\varepsilon}^{(1)} + I_{\varepsilon}^{(2)}, \tag{B7}$$

with

$$I_{\varepsilon}^{(1)} = -ik^{0}\int dx^{-}h(k^{0}x^{-})e^{-i[H(k^{0}x^{-}) + Q^{+}x^{-}] - \varepsilon|x^{-}|}, \tag{B8}$$

and

$$I_{\varepsilon}^{(2)} = -\varepsilon\int dx^{-}\mathrm{sgn}(x^{-})e^{-i[H(k_{0}x^{-}) + Q^{+}x^{-}] - \varepsilon|x^{-}|}. \tag{B9}$$

Since the integral $I_{\varepsilon}^{(1)}$ is over the finite region such that $\Phi^{0}/k^{0} \leqslant x^{-} \leqslant \Phi/k^{0}$, we can put there $\varepsilon = 0$. In the second integral we divide the integration space into three regions, $(-\infty,\Phi^{0}/k^{0}]$, $[\Phi^{0}/k^{0},\Phi/k^{0}]$, and $[\Phi/k^{0},\infty)$.

This leads us to

$$I_\varepsilon^{(2)} = \theta(-\Phi_0)e^{(\varepsilon - iQ^+)\Phi^0/k^0}\frac{\varepsilon}{\varepsilon - \mathrm{i}Q^+} + \theta(\Phi_0)\left[\frac{\varepsilon}{\varepsilon - iQ^+} + \frac{\varepsilon}{\varepsilon + iQ^+}\left(e^{-(\varepsilon + iQ^+)\Phi^0/k^0} - 1\right)\right]$$
$$- \varepsilon\int_{\Phi^0/k^0}^{\Phi/k^0} dx^-\mathrm{sgn}(x^-)e^{-i[H(k^0x^-)+Q^+x^-]-\varepsilon|x^-|} + \theta(-\Phi)e^{-iH(\Phi)}\left[\frac{\varepsilon}{\varepsilon - iQ^+}\left(1 - e^{(\varepsilon - iQ^+)\Phi^0/k^0}\right) - \frac{\varepsilon}{\varepsilon + iQ^+}\right]$$
$$- \theta(\Phi)e^{-iH(\Phi)-(\varepsilon + iQ^+)\Phi/k^0}\frac{\varepsilon}{\varepsilon + iQ^+}, \tag{B10}$$

where $\theta(\Phi)$ is the step function. As one can see, this integral in the limit when $\varepsilon \to 0$ vanishes provided that $Q^+ \neq 0$. Since from the condition $\delta^{(1)}(Q^-)$ we have also $Q^0 = Q^\parallel$, we conclude that $Q^+ = Q^0 \neq 0$. Finally, we obtain

$$\int d^4x\, e^{-iH(k\cdot x)-iQ\cdot x} = -\frac{k^0}{Q^0}\int d^4x\, h(k\cdot x)e^{-iH(k\cdot x)-iQ\cdot x}, \tag{B11}$$

which holds only if $Q^0 \neq 0$. This is an analog of the transformation derived by Boca and Florescu in Ref. [20].

[1] S. Araki *et al.*, KEK Report No. 2005-60, CLIC note 639, LAL 05-94 (arXiv:physics/0509016v2 [physics.acc-ph]).
[2] E. Bulyak, P. Gladkikh, V. Skomorokhov, T. Omori, J. Urakawa, K. Moenig, and F. Zimmermann, Phys. Rev. ST Accel. Beams **9**, 094001 (2006).
[3] Super B Conceptual Design Report No. INFN/AE-07/2, SLAC-R-856, LAL 07-15 (arXiv:0709.0451v2 [hep-ex]).
[4] A. H. Compton, Phys. Rev. **21**, 483 (1923).
[5] A. H. Compton, Phys. Rev. **22**, 409 (1923).
[6] R. H. Milburn, Phys. Rev. Lett. **10**, 75 (1963).
[7] F. R. Arutyunian, Phys. Lett. **4**, 176 (1963).
[8] A. I. Nikishov and V. I. Ritus, Zh. Eksp. Teor. Fiz. **46**, 776 (1963) [Sov. Phys. JETP **19**, 529 (1964)]; Zh. Eksp. Teor. Fiz. **46**, 1768 (1964) [Sov. Phys. JETP **19**, 1191 (1964)]; Zh. Eksp. Teor. Fiz. **47**, 1130 (1964) [Sov. Phys. JETP **20**, 757 (1965)].
[9] N. B. Narozhny, A. I. Nikishov, and V. I. Ritus, Zh. Eksp. Teor. Fiz. **47**, 930 (1964) [Sov. Phys. JETP **20**, 622 (1965)].
[10] L. S. Brown and T. W. B. Kibble, Phys. Rev. **133**, A705 (1964).
[11] I. I. Goldman, Phys. Lett. **8**, 103 (1964).
[12] F. Ehlotzky, K. Krajewska, and J. Z. Kamiński, Rep. Prog. Phys. **72**, 046401 (2009).
[13] P. Panek, J. Z. Kamiński, and F. Ehlotzky, Phys. Rev. A **65**, 033408 (2002); Opt. Commun. **213**, 121 (2002); Eur. Phys. J. D **26**, 3 (2003).
[14] D. Yu. Ivanov, G. L. Kotkin, V. G. Serbo, Eur. Phys. J. C **36**, 127 (2004).
[15] C. Harvey, T. Heinzl, and A. Ilderton, Phys. Rev. A **79**, 063407 (2009).
[16] A. Hartin and G. Moortgat-Pick, Eur. Phys. J. C **71**, 1729 (2011).
[17] R. A. Neville and F. Rohrlich, Phys. Rev. D **3**, 1692 (1971).
[18] N. B. Narozhny and M. S. Fofanov, Zh. Eksp. Teor. Fiz. **110**, 26 (1996) [Sov. Phys. JETP **83**, 14 (1996)].
[19] S. P. Roshchupkin, A. A. Lebed', E. A. Padusenko, and A. I. Voroshilo, in *Quantum Optics and Laser Experiments*, edited by S. Lyagushyn (InTech, Rijeka, 2012), p. 107.
[20] M. Boca and V. Florescu, Phys. Rev. A **80**, 053403 (2009).
[21] T. Heinzl, D. Seipt, and B. Kämpfer, Phys. Rev. A **81**, 022125 (2010).
[22] F. Mackenroth, A. Di Piazza, and C. H. Keitel, Phys. Rev. Lett. **105**, 063903 (2010).
[23] D. Seipt and B. Kämpfer, Phys. Rev. A **83**, 022101 (2011).
[24] F. Mackenroth and A. Di Piazza, Phys. Rev. A **83**, 032106 (2011).
[25] M. Boca and V. Florescu, Eur. Phys. J. D **61**, 449 (2011).
[26] Y. Y. Lau, F. He, D. P. Umstadter, and R. Kowalczyk, Phys. Plasmas **10**, 2155 (2003).
[27] D. Umstadter, J. Phys. D **36**, R151 (2003).
[28] T. J. Englert and E. A. Rinehart, Phys. Rev. A **28**, 1539 (1983).
[29] C. I. Moore, J. P. Knauer, and D. D. Meyerhofer, Phys. Rev. Lett. **74**, 2439 (1995).
[30] C. Bula, K. T. McDonald, E. J. Prebys, C. Bamber, S. Boege, T. Kotseroglou, A. C. Melissinos, D. D. Meyerhofer, W. Ragg, D. L. Burke, R. C. Field, G. Horton-Smith, A. C. Odian, J. E. Spencer, D. Walz, S. C. Berridge, W. M. Bugg, K. Shmakov, and A. W. Weidemann, Phys. Rev. Lett. **76**, 3116 (1996).
[31] C. Bamber, S. J. Boege, T. Koffas, T. Kotseroglou, A. C. Melissinos, D. D. Meyerhofer, D. A. Reis, W. Ragg, C. Bula, K. T. McDonald, E. J. Prebys, D. L. Burke, R. C. Field, G. Horton-Smith, J. E. Spencer, D. Walz, S. C. Berridge, W. M. Bugg, K. Shmakov, and A. W. Weidemann, Phys. Rev. D **60**, 092004 (1999).
[32] D. M. Volkov, Z. Phys. **94**, 250 (1935).
[33] K. Krajewska and J. Z. Kamiński, Phys. Rev. A **82**, 013420 (2010).
[34] D. B. Milošević, G. G. Paulus, D. Bauer, and W. Becker, J. Phys. B **39**, R203 (2006).
[35] K. Krajewska and J. Z. Kamiński, Phys. Rev. A **85**, 043404 (2012).
[36] G. A. Mourou, T. Tajima, and S. V. Bulanov, Rev. Mod. Phys. **78**, 309 (2006).
[37] T. Heinzl, A. Ilderton, and M. Marklund, Phys. Lett. B **692**, 250 (2010).